JOURNAL OF MATERIALS SCIENCE 27 (1992) 3869–3875

Role of zirconium in the phase formation at the interdendritic zone in nickel-based superalloys

E. GOZLAN, M. BAMBERGER, S. F. DIRNFELD
Department of Materials Engineering, Technion, Haifa, Israel

B. PRINZ
Metallgesellschaft AG, Postfach 101 501, Frankfurt, Germany

A commercial Alloy 80A and a modified alloy with lower titanium and zirconium contents, e.g. 1.4% and < 0.01%, respectively, were subjected to unidirectional solidification followed by a rapid quench in water to preserve the structure at elevated temperatures. The slow solidification results in a coarse dendritic structure with a high enrichment of sulphur (up to 2%), aluminium (up to 4%), titanium (up to 13%) and zirconium in the interdendritic zones. In the commercial Alloy 80A, the zirconium and sulphur present in the interdendritic zone result in a eutectic containing ZrS and NiCrTi-matrix. Excess zirconium forms an NiZr-intermetallic. No TiS is formed in this case. In the absence of zirconium, the titanium enriched in the interdendritic residual melt forms a eutectic of TiS. In both cases the effective solidus temperature corresponding to the composition of the residual melt is 1170°C, compared to 1330°C, which is the solidus temperature of the bulk material.

1. Introduction

Nickel-based superalloys used at elevated temperatures present a severe problem in segregation during solidification. By the nature of their design applications, these materials must be uniform and homogeneous to a high degree in order to ensure performance, yet, due to their highly alloyed constitutions they are among the most segregation-prone of all industrial metallic systems. Moreover, large ingot castings are increasingly prone to segregation of the alloying elements [1–4] and impurities [5]. The segregation of alloying elements such as molybdenum, aluminium and tantalum is the origin of "Freckles" or TCP phases formed in the enriched interdendritic zones, whereas the segregation of impurities, such as sulphur results in grain-boundary embrittlement [4]. These intermetallics and sulphides are not dissolved in the γ-matrix during the subsequent homogenization and hot forming. Furthermore, these treatments are made more difficult by the fact that at the same time the effective solidus temperature is reduced.

The solidification behaviour can be strongly influenced even by quite small additions of alloying elements. In this respect experience has shown that, in the case of the Alloy 80A superalloy, special significance attaches to the zirconium content which, as a rule, amounts to < 0.1%.

It was the object of the present investigation to clarify the effect of low zirconium contents on the alloying behaviour of the different alloying elements, as well as on the phase composition of Alloy 80A. In addition, the suitability of the experimental method of "interrupted directional solidification" was tested to ascertain its effectiveness in investigations into the crystallization behaviour and the influence of individual alloying elements.

2. Experimental procedure

Several batches of Alloy 80A with slight compositional modifications were vacuum-induction melted, cast into billets, and hot-forged to bars of 12.5 mm diameter. The compositions of the different lots are listed in Table I. The solidification behaviour of these materials was investigated by interrupted directional solidification (IDS).

The experimental apparatus and conditions of investigations involving IDS have already been described in detail [6]. The temperature of the melt was 1500 °C, the speed of withdrawal 50 mm h^{-1}. In the experimental conditions applying here the resulting temperature gradient, G, at the solidification front was 90 K cm^{-1} [6], hence the quotient, G/R = 18 Kh cm^{-2}. Based on a comparison with G/R values given in earlier works [4, 6], a dendritic morphology of solidification can be expected.

After about 1 h directional solidification the specimens were water-quenched in order to obtain a fine dendritic solidification of the residual melt.

Because the metallographic and microanalytical evaluations showed the interdendritic zones to have been very considerably enriched in alloying elements,

0022–2461 © *1992 Chapman & Hall*

button-shaped specimens were prepared by vacuum-arc melting in order to determine the effective solidus temperatures of such residual melts and to characterize their as-cast structure.

3. Results

Fig. 1 shows the longitudinal cross-section of Specimen 1 after the IDS process and slightly etching with Kalling solution. The microphotograph clearly shows the situation at the solidification front. In stationary conditions the solidification is attended by a relatively coarse dendritic growth depending on the experimental parameters selected. The melt ahead of the solidification front and in the interdendritic regions of the solidified zone exhibited a very fine structure due to the rapid quenching.

As the distance from the solidification front increased, the share of the residual melt decreased very rapidly. As close as 0.5 cm behind the solidification front, metallographic methods are unable to determine to what extent interdendritic regions were still liquid at the time of quenching, or if they had already solidified.

The thermal conditions at the liquid/solid phase boundary have been reconstructed as shown in Fig. 1.

(a) The solidification front indicates the site of the liquidus isotherms; the liquidus temperature of the Alloy 80A was determined by thermal analysis to be 1370 °C. The progress of the temperature at both faces of the solidification front is given by the temperature gradient calculated in [6]. Any deformation of the solidification bath (the heterogeneous region solid/liquid) as a result of liberated heat of solidification and

TABLE I Modified Alloys 80A

	Cr	Fe	Co	Si	Ti	Zr	Al	S	P	C	Mg
1	19.4	0.03	1.1	0.09	2.33	0.05	1.38	0.003	0.005	0.041	0.008
2	20.0	0.03	1.1	0.04	1.38	< 0.01	1.48	0.003	0.005	0.033	0.006

Mo, Mn and Nb content less than 0.01%.

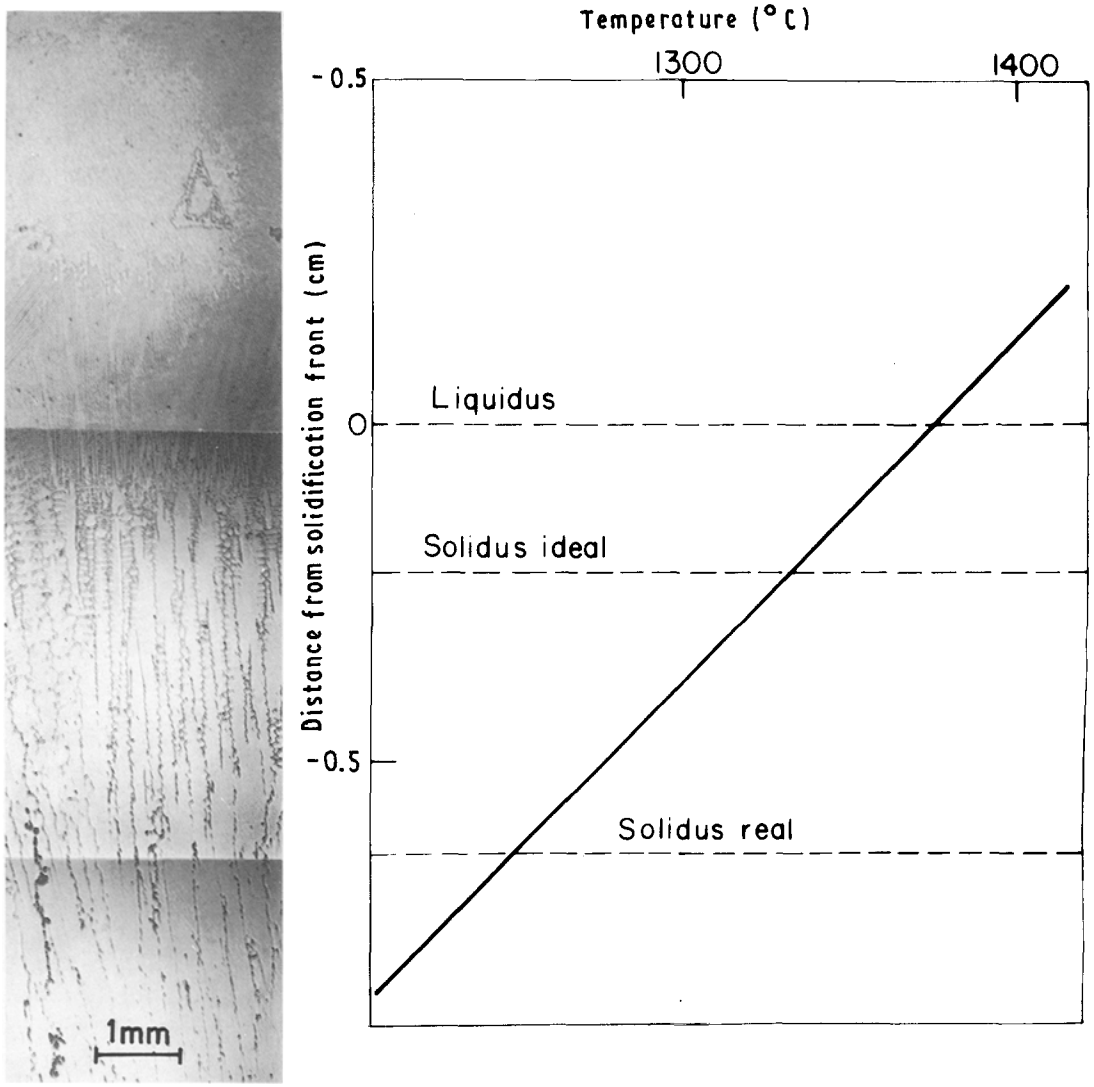

Figure 1 Longitudinal cross-section of Specimen 1 and the corresponding temperatures along the axis.

altered heat conductivity, can be neglected, which is permissible considering the low rate of solidification.

(b) The equilibrium solidus temperature, $T_{s-ideal}$, has been measured by differential thermal analysis (DTA) and found to be 1330 °C. However, the solidified structure of Fig. 1 shows that at the site of the solidus isotherm, $T_{s-ideal}$, solidification was by no means completed, so that the actual solidification zone was about three times as wide.

(c) In the melt, serrated precipitates are discerned,

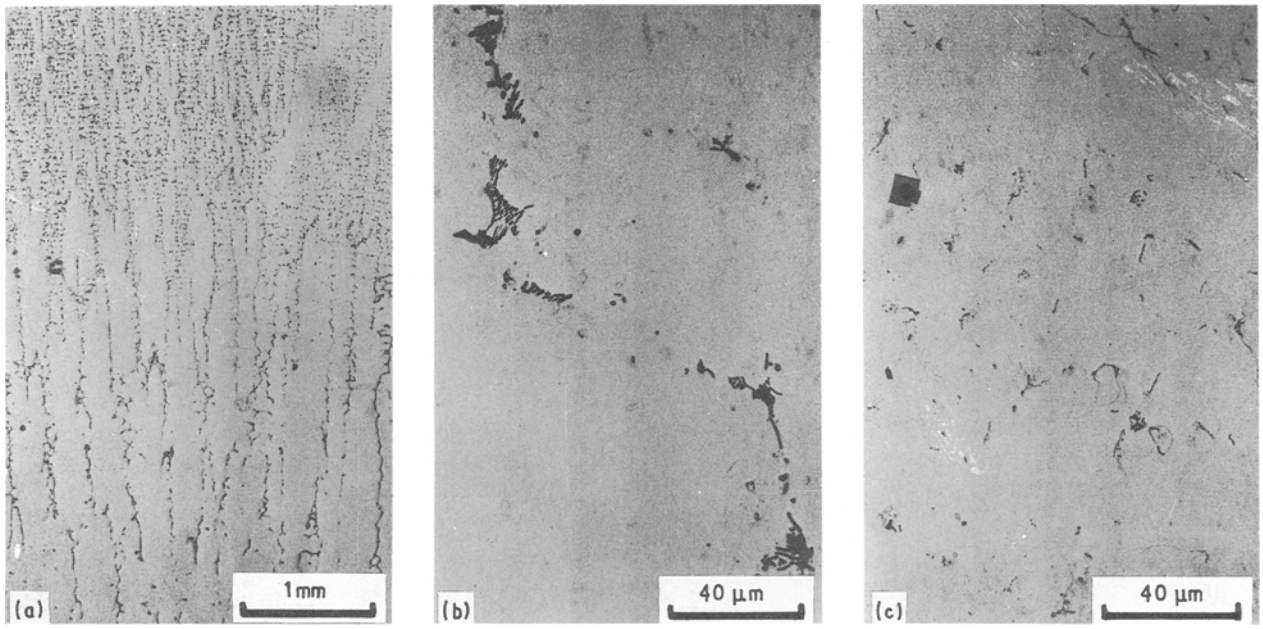

Figure 2 Longitudinal cross-section of Specimen 2. (a) Low magnification, (b) the solid, and (c) the melt ahead the solidification front.

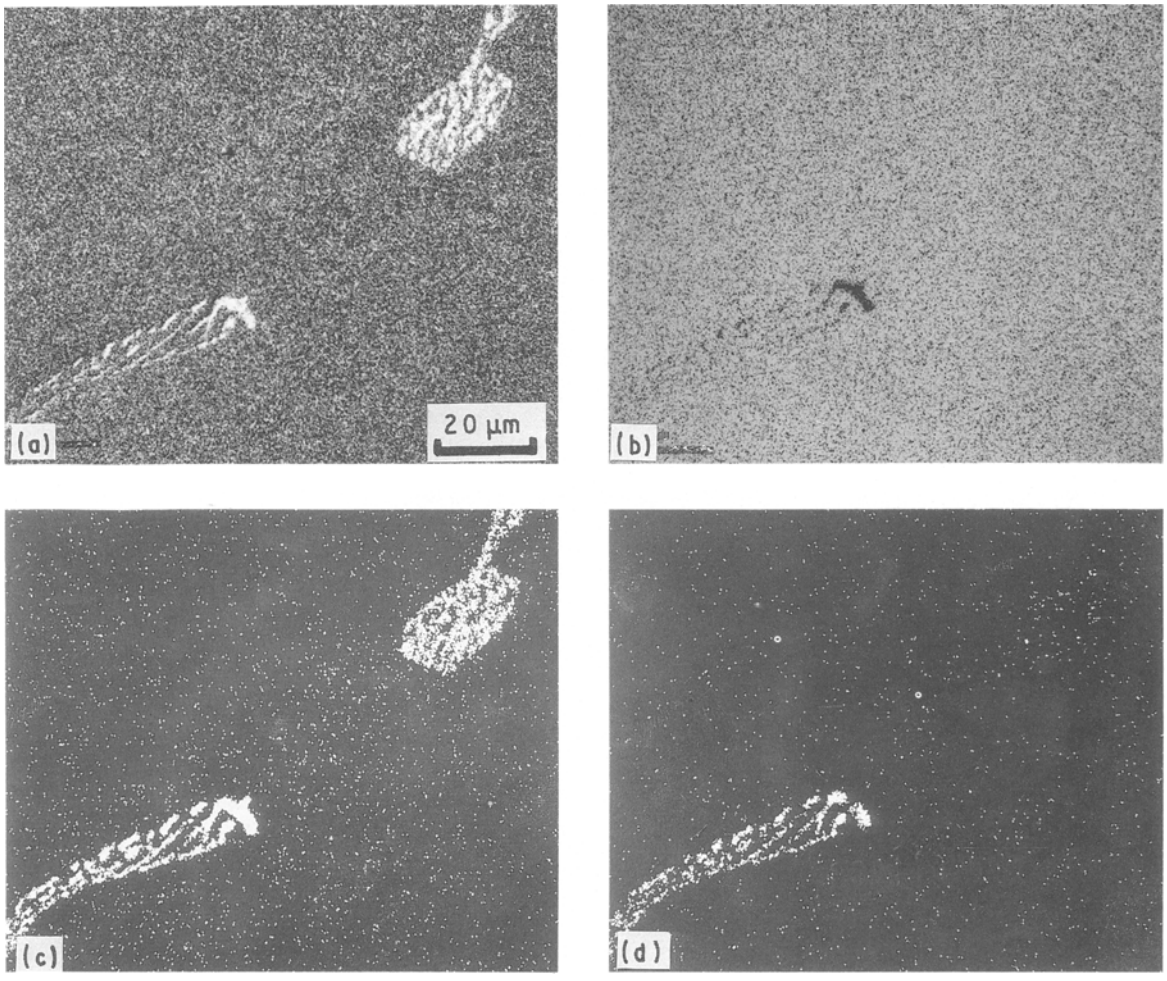

Figure 3 The interdendritic residual melt in Specimen 1. (a) Reflected electron picture, (b) X-ray mapping of nickel, (c) X-ray mapping of zirconium, and (d) X-ray mapping of sulphur.

which contain TiC with the morphology characteristic of titanium–carbon nitrides Ti(C, N). At temperatures above 1400 °C, these primary precipitates appear long before the phase boundary is reached. As the temperature decreases, the amount of primary precipitates increases. In front of the phase boundary, agglomeration is evident. In the solid state, some of the primary precipitates are arranged in lines in the direction of crystallization, without co-ordination with grain or subgrain boundaries.

Fig. 2a shows Specimen 2, etched and longitudinally polished, in low magnification. In the lower half of the picture the coarse dendritic directional solidification can be seen. Above it, clearly delimited, is a very fine dendritic structure, forcibly achieved by water quenching of the melt ahead of the solidification front.

In addition to yellow–orange coloured angular and, in part, oddly shaped inclusions in the dendrites (presumably titanium carbonitrides) eutectically precipitated grey and light-grey needles and platelets can be found in the interdendritic zones (Fig. 2b). Here and there fine grain-boundary overlays can be observed. In the fine dendritic solidified melt (Fig. 2c) the eutectic precipitated in the interdendritic regions is substantially more finely textured and less enriched. The yellow–orange coloured inclusions are present only in angular plate-like shape. Other "oddly shaped" inclusions could not be found in this area. In the melt zone, too, fine overlays are here and there observed on the grain boundaries.

Specimen 1 generally shows a similar structure, although the interdendritic enrichment of the residual melt by alloying elements appears to be higher.

Fig. 3a is a reflected-electron picture of the interdendritic residual melt of Specimen 1. Two typical kinds of eutectic are discernible: one consisting of Ni–Cr–Ti matrix with lamellar ZrS as a secondary phase (Fig. 3a below, left), the other containing Ni–Zr as secondary phase, as can be deduced from the X-ray mapping of nickel, zirconium and sulphur given in Fig. 3b–d, respectively. In addition, intermetallic phases, rich in zirconium and carbon but lacking nickel and chromium and with little titanium and sulphur, were detected. These appear to be carbides of zirconium.

Fig. 4a is a reflected-electron picture of a typical eutectic containing TiS as secondary phase (see Fig. 4c and d), in which some chromium and zirconium are dissolved. Despite the low zirconium content a local precipitate rich in zirconium and carbon was found at the edge of the eutectic – apparently zirconium

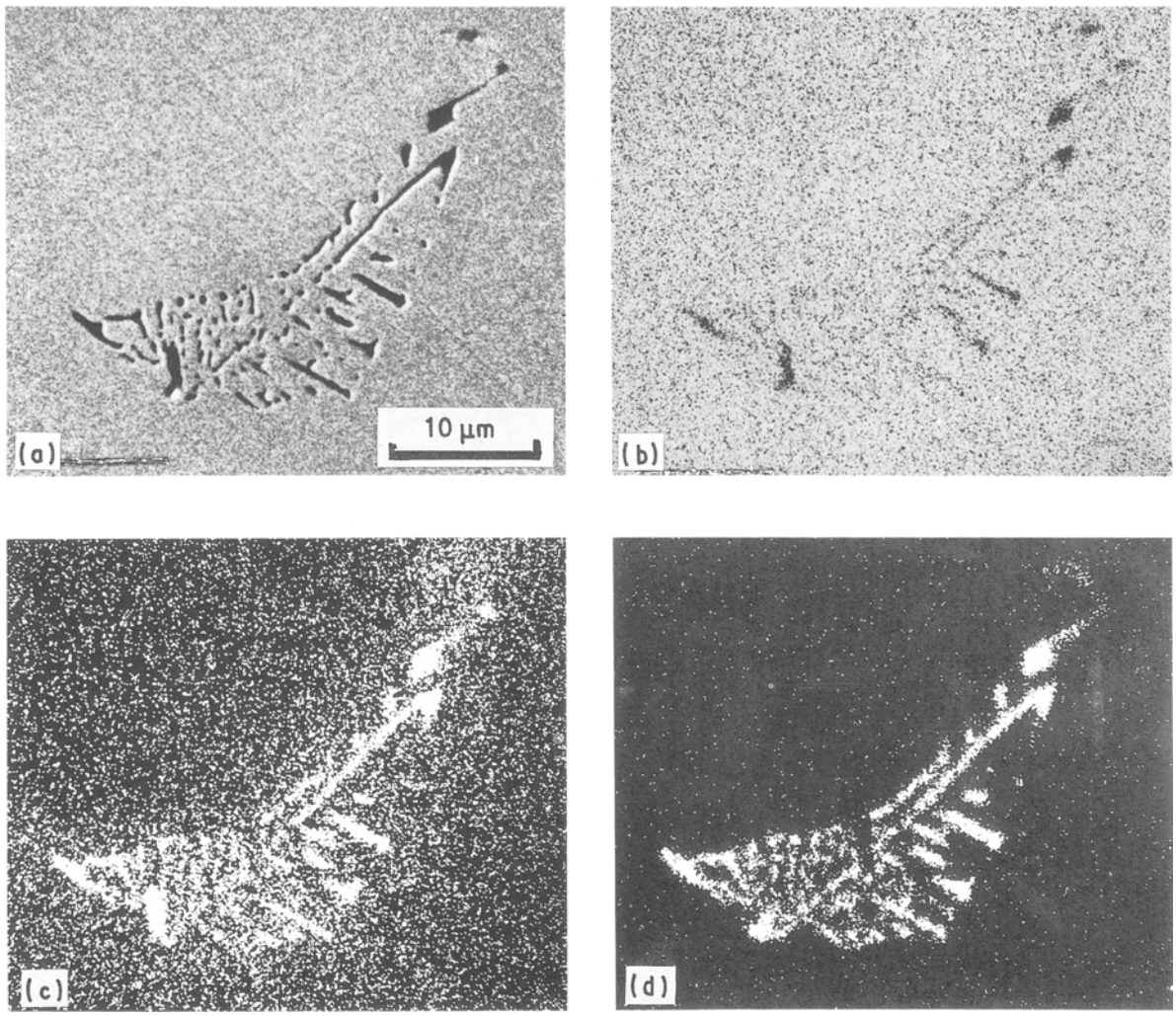

Figure 4 The interdendritic residual melt in Specimen 2. (a) Reflected electron picture, (b) X-ray mapping of nickel, (c) X-ray mapping of titanium and (d) X-ray mapping of sulphur.

carbides. Furthermore titanium carbonitrides and Ti-Zr–Cr-sulphides were observed. The approximate chemical composition of the interdendritic residual melt is 64% Ni, 19% Cr, 13% Ti, 4% Al, and 2% S. Two specimens of that composition were prepared by vacuum arc melting, one with, the other without, sulphur. These specimens were re-melted in a resistance furnace and then subjected to slow cooling.

The structure of the specimen of a composition equal to that of the residual melt (but without sulphur) is depicted in Fig. 5. In addition to the bright primary precipitates, in dendrite-shaped or round section depending on the orientation, a fine to very fine eutectic is discernible.

The specimen with the composition of the residual melt (Specimen 2 with sulphur) exhibits a structure markedly different from that of the sulphur-free specimen (Fig. 6). A fine multi-phase eutectic, consisting of fine bright rounded precipitates, is observed, as well as yellow–orange coloured predominantly needle-shaped phases.

The specimens with the composition of the residual

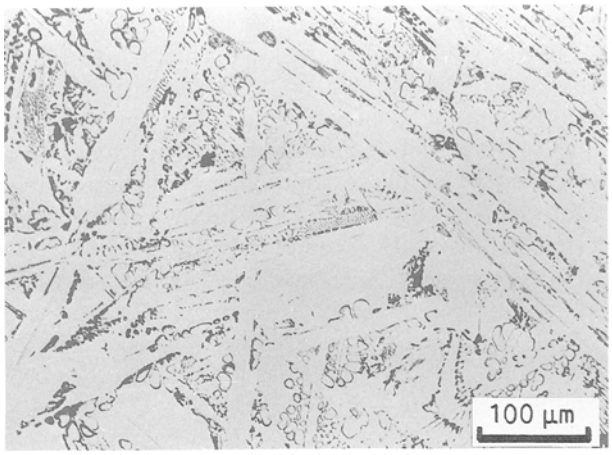

Figure 5 Microstructure of sulphur-free sample following slow cooling.

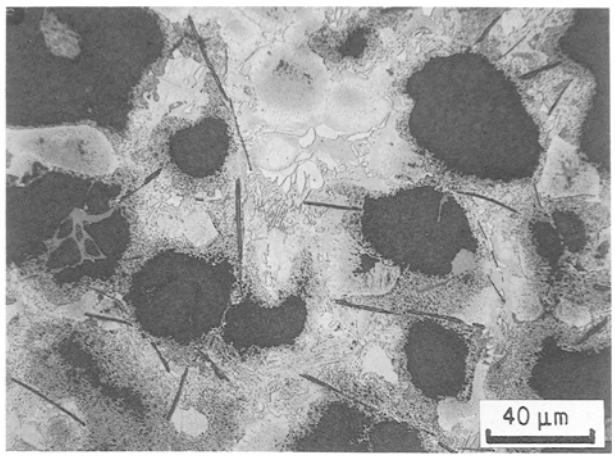

Figure 6 Microstructure of sample corresponding the residual melt composition following slow cooling.

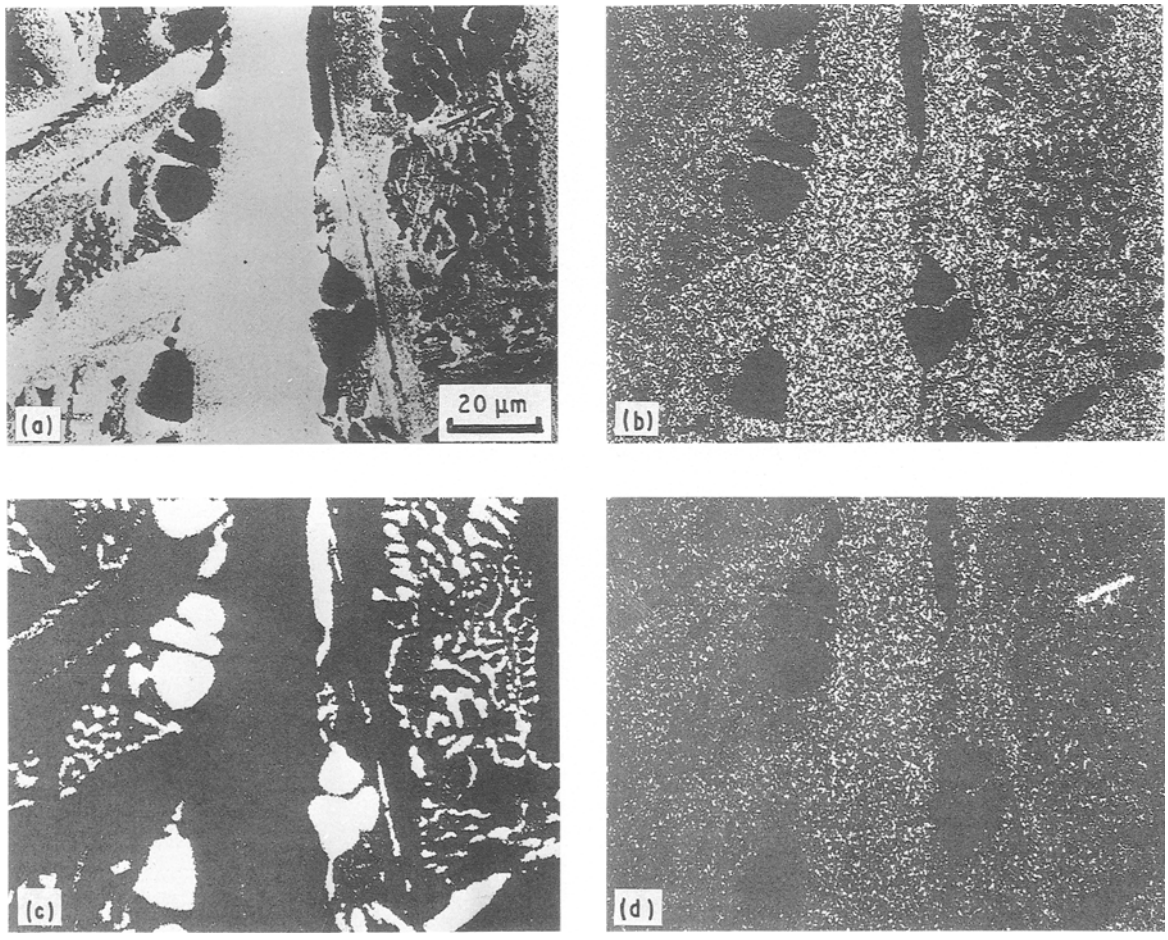

Figure 7 The sulphur-free sample. (a) Reflected electron picture, (b) X-ray mapping of nickel, (c) X-ray mapping of chromium, and (d) X-ray mapping of titanium.

melt of Specimen 2 (without and with sulphur) exhibit a complex phase composition under the microprobe. The sulphur-free specimen exhibits, in the first instance, three main components, as seen in the distribution pictures (Fig. 7): a phase containing nickel, titanium and small quantities of chromium and aluminium (nickel-phase); a chromium-containing phase (chromium-phase) lodged in the above; a phase of higher aluminium content, in which small amounts of nickel, titanium and chromium are dissolved (aluminium phase). The probe with a 2% addition of sulphur (Fig. 8) contains, in the Ni, Cr, Ti, Al-matrix, a chromium-rich eutectic and titanium-sulphide needles. The thermal analysis of the sulphur-free residual melt clearly shows that at least two phases solidify. At approximately 1200 °C the nickel-phase (Ni–Ti–Al) crystallizes to all appearances, closely followed, at about 1170 °C, by a eutectic from the chromium and the aluminium-phase.

The solidification sequence of the same melt but with an addition of 2% S, on the other hand, appears to be much more complex. According to the results of the DTA, at least four different phases should precipitate in the temperature range between 1250 and 1170 °C. A comparison between the results of DTA and those of the microprobe in Fig. 8 indicates that at about 1250 °C TiS is formed first of all, i.e. before the nickel-phase and a eutectic solidify at 1170 °C. From this it is concluded that the solidus temperature of the residual melt is by no means higher than 1250 °C, compared with 1330 °C of the regular 80A alloy. This is, then, the temperature at which solidification is almost completed, and it is therefore called T_{s-real} in Fig. 1. There is good agreement between the location of that temperature and the end of solidification seen in the metallographic picture.

4. Discussion

The investigations provide indications of the crystallization behaviour of complex alloys and dissolved elements, which cannot be obtained in any other way, because the phase equilibria are not known.

Nitrogen dissolved in the melt is emitted early, far above the liquidus temperature, exclusively in the form of titanium nitride or titanium carbonitride (this applies to both alloys examined). The zirconium does not take part in this reaction. Despite the lower free-energy associated with the formation of ZrN ($G^{1400\,°C}_{ZrN}$ $= -102$ kcal mol^{-1}) compared with TiN ($G^{1400\,°C}_{TiN}$ $= -92$ kcal mol^{-1}) [7] the ZrN is not formed due to the low zirconium content. In front of the phase boundary, some of the precipitated TiN agglomerates and is therefore found irregularly distributed over the solidified structure.

In the alloy variant containing zirconium the residual melt becomes highly enriched with zirconium, which is finally precipitated as ZrS. TiS was not found

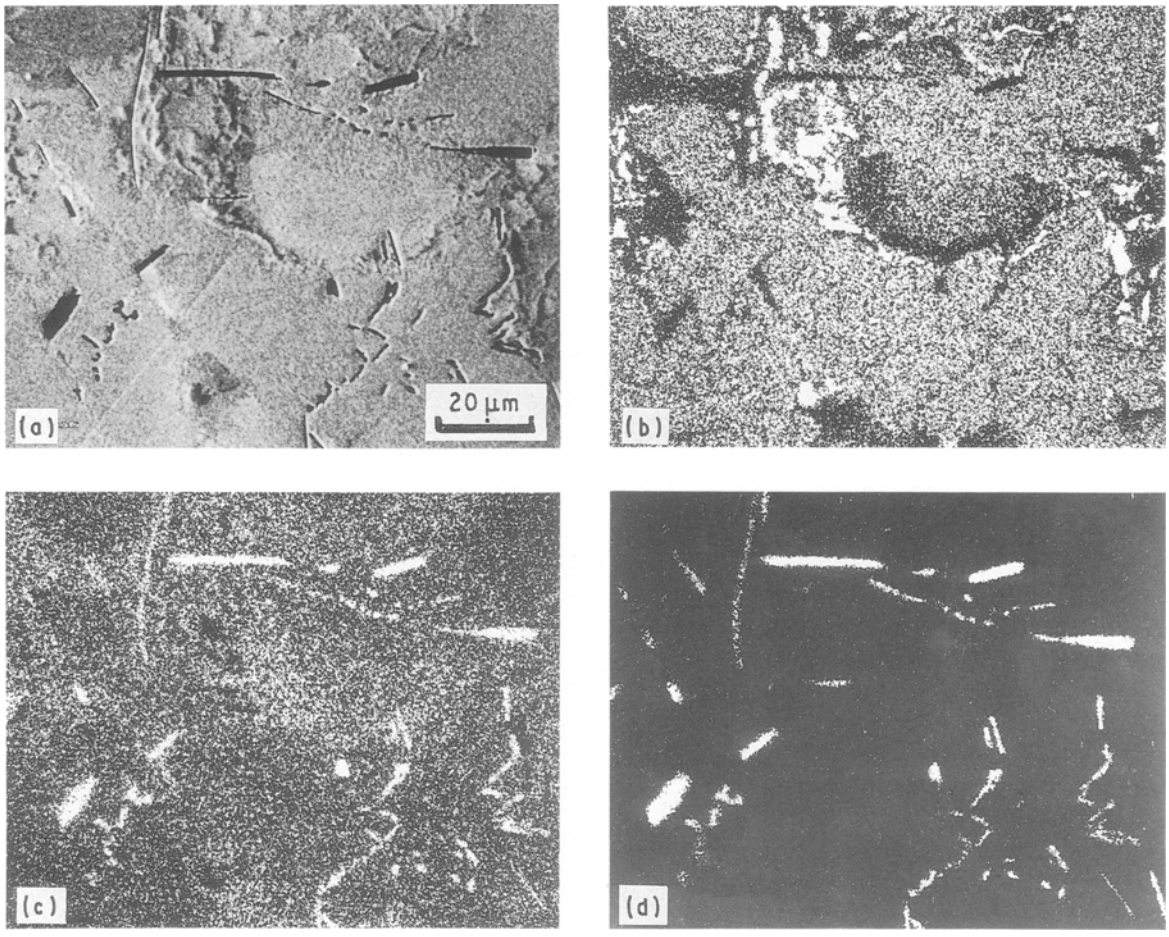

Figure 8 The sample corresponding the residual melt composition. (a) Reflected electron picture, (b) X-ray mapping of chromium, (c) X-ray mapping of titanium, and (d) X-ray mapping of sulphur.

when zirconium was present. In the γ-matrix, zirconium is dissolved only in undetectable amounts. Hence, the distribution coefficient of zirconium is extremely small. Excess zirconium, not bonded as ZrS, forms an intermetallic phase with nickel and titanium. ZrS and the intermetallic zirconium-phase solidified eutectically together with γ at a low temperature.

In the absence of zirconium, enriched sulphur is precipitated in the form of TiS in the residual melts. Sulphur enrichment up to about 2% takes place in the eutectically solidifying residual melt, together with titanium (~ 13%) and aluminium (~ 4%).

Based on the assumption of solidification in accordance with the Scheil model [8] and an equilibrium distribution coefficient for titanium, $k^{\circ}_{Ti} = 0.4$, which corresponds to the results of previous investigations [3, 4], an estimate is arrived at that titanium enrichment up to 13% in the residual melt should ensue after crystallization of 95% of the melt volume. The share of the eutectically solidified residual melt detectable in the structure is, however, clearly smaller; in other words, the distribution coefficients change as enrichment increases. In any case the distribution coefficients for sulphur must be extremely small in order that the high degrees of enrichment measured be feasible. They cannot, however, be measured with the available methods.

In the absence of zirconium, titanium is bonded to sulphur, and the effective amount for the creation of γ′ is smaller than designed. An addition of zirconium, however small, binds the sulphur and leaves the titanium free to form γ′. Different intermetallic phases besides sulphides are formed out of the enriched residual melts, as is made manifest in the structure and in the phase transitions observed in specimens having a composition similar to that of the residual melt. By enrichment with alloying elements the effective solidus temperature is reduced to about 1170 °C (equilibrium solidus temperature 1330 °C).

The high local content of alloying elements and impurities at the interdendritic zones leads to the appearance of brittle phases that do not decompose during homogenization and may, therefore, cause difficulties when the billets are rolled. In addition, the effective solidus temperature is very low, so that homogenization or solution treatment at 1200 °C is liable to cause the grain boundaries to melt, leading to the disintegration of the billet during rolling.

5. Conclusions

1. The slow solidification of Alloy 80A results in segregation of titanium, sulphur and zirconium in the interdendritic zones, forming ZrS and an NiZr phase.

2. In an alloy with a lower content of titanium and the absence of Zr, TiS is eutectically solidified in the interdendritic zones. This, in turn, results in lower γ′ precipitation due to lower content of titanium dissolved in the γ matrix.

3. The solidification temperature of the eutectic is 1170 °C compared to 1330 °C, the solidus temperature of the bulk material.

4. The heat treatment window for homogenization is thus narrower than can be expected based on the DTA analysis.

Acknowledgement

The research was promoted by the Federal Ministry for Research and Technology, Bonn, within the programme "German–Israel Cooperation in the field of High-Temperature Materials" (Project no. 03 M 3003 A7).

References

1. J. A. DOMINGUE, R. O. YU and H. D. FLANDERS, in Conference Proceedings, Cleaveland, OH, 12–13 September 1984 (NASA C1 2337) pp.139–49.
2. J. LACAZE, A. CHEHAIBOU and G. LESOULT, *Z. Metallkde* **80** (1989) 15.
3. B. PRINZ and G. RUDOLPH, *Mikrochim. Acta (Wien) Suppl.* **11** (1985) 275.
4. D. MA and P. R. SAHM, *Giessereiforschung* **42** (1990) 122.
5. R. H. BRICKNELL, R. A. MULFORD and D. A. WOODFORD, *Met. Trans.* **13A** (1982) 1223.
6. M. BAMBERGER, S. F. DIRNFELD and Y. ZUTA, *J. Cryst. Growth* **73** (1985) 142.
7. B. MARINCEK, *Metall.* **31** (1977) 627.
8. M. C. FLEMINGS, "Solidification Processing" (McGraw-Hill, New York, 1974).

Received 25 March
and accepted 1 July 1991